ChemPubSoc Europe

DOI: 10.1002/cphc.201800389

CHEMPHYSCHEM Articles

Special Issue

Ternary Polymeric Composites Exhibiting Bulk and Surface Quadruple-Shape Memory Properties

Shelby L. Buffington,[a, b] Benjamin M. Posnick,[b] Justine Paul,[a, b] and Patrick T. Mather*[a, b, c]

We report the design and characterization of a multiphase quadruple shape memory composite capable of switching between 4 programmed shapes, three temporary and one permanent. Our approach combined two previously reported fabrication methods by embedding an electrospun mat of PCL in a miscible blend of epoxy monomers and PMMA as a composite matrix. As epoxy polymerization occurred the matrix underwent phase separation between the epoxy and PMMA materials. This created a multiphase composite with PCL fibers and a two-phase matrix composed of phase-separated epoxy and PMMA. The resulting composite demonstrated three separate thermal transitions and amenability to mechanical programming of three separate temporary shapes in addition to one final, equilibrium shape. In addition, quadruple surface shape memory abilities are successfully demonstrated. The versatility of this approach offers a large degree of design flexibility for multi-shape memory materials.

1. Introduction

Shape memory polymers (SMPs) are a special class of materials that can store one or more temporary shapes and macroscopically transition from a stored shape to a permanent, "remembered" shape in response to an external stimulus.[1] Such behavior requires two components: a memory component (phase or macromolecular constituent) that can be in the form of physical or chemical cross-links, crystalline domains, or interpenetrating networks; and a shape-fixing component (phase or macromolecular constituent) that can come from either crystallization, vitrification, liquid crystal transitions, reversible molecular cross-linking and supramolecular associations.[2,3] In a typical shape memory cycle (SMC), the SMP is heated above a characteristic transition temperature to a compliant, rubbery state. An external stress is then applied to the material, resulting in deformation to a new, temporary shape with mechanical resistance from the memory component of the material. This deformation – often termed "mechanical programming" – decreases the polymer network's configurational entropy to an unfavorable state which is locked in when the material is cooled below its transition temperature and the constituent network chains of the memory phase are immobilized. Once heated above this transition temperature, however, the network chains are remobilized so that rubber (entropy) elasticity acts to return the object toward its permanent shape.[2–4]

SMPs with a wide range of material properties have been designed and are reviewed briefly here for the interested reader.[1–3,5–7] Due to inherent versatility, SMPs have been proposed for applications spanning biomedical devices,[8,9] space applications, microsensors and actuators, drug delivery systems and intelligent textiles, among others.[1,3] The most common trigger for a SMP is heat; however, SMPs triggered by light[10,11] ultrasound,[12] electricity,[13] water[14,15] solvents[16] and magnetism[17,18] have been reported as well. SMPs exhibiting unique properties like anisotropy,[19] soft actuation,[20] light emission,[21] self-healing[22] and other special properties reviewed here[23] have also been developed. In addition, SMPs with reconfigurable permanent shapes have been introduced, allowing the possibility that the SMP could be mass-produced but with the permanent shape being amenable to reprogramming as desired for specific applications.[24,25] SMPs that can reversibly actuate between their permanent and temporary shape, called reversible SMPs, have also been proposed for applications involving switches and actuators,[26,27] for instance, soft muscle actuators.[28]

An important limitation of the described SMP systems is that most are only able to fix one shape, yielding limited actuation between just two shapes: one fixed (or "programmed") and one permanent. Multi-shape memory polymers (multi-SMPs) are capable of being programmed into at least two temporary shapes while possessing one permanent shape which allow the materials to undergo more complex shape changes.[6] The first example of a triple shape memory (TSM) material was designed by Bellin and co-workers who combined two crystalline switching segments, poly(ε-caprolactone) (PCL) and poly(ethylene glycol) (PEG) within the context of a polymer network.[29] Since this development, two primary methods for producing multi-shape memory materials have been employed.

[a] S. L. Buffington, J. Paul, Dr. P. T. Mather
Biomedical and Chemical Engineering Department
Syracuse University
Syracuse, NY 13244 USA
E-mail: patrick.mather@bucknell.edu
[b] S. L. Buffington, B. M. Posnick, J. Paul, Dr. P. T. Mather
Syracuse Biomaterials Institute
Syracuse University
Syracuse, NY 13244 USA
[c] Dr. P. T. Mather
Chemical Engineering Department
Bucknell University
Lewisburg, PA 17837 USA

Supporting information for this article is available on the WWW under https://doi.org/10.1002/cphc.201800389

An invited contribution to a Special Issue on Smart Materials

The first is combining materials with separate thermal transitions in either a macromolecular chemistry or by blending two or more polymers in a composite approach. For example, our group designed a triple shape polymeric composite by embedding a PCL fiber mat into an epoxy-based SMP matrix.[30] This created a composite with two interpenetrating phases – with separate thermal transitions – capable of fixing two temporary shapes. In addition, our group developed a triple shape composite using polymerization induced phase separation (PIPS).[31] In this method, epoxy monomers and low molecular weight PCL were mixed into a single phase melt that, upon polymerization, underwent phase separation to create an SMP matrix with pockets of PCL distributed throughout the material. Using a similar method we also designed the first example of triple shape composite foams,[32] while other groups have expanded the abilities of multi-shape materials by designing systems that respond to different triggers, such as pH,[33] light[33] and magnetism.[34]

Another approach to make multi-SMPs involves materials with distinctly broad glass transitions that allows one glass transition event (albeit broad) to mechanically program multiple shapes at different temperatures within the transition and to recover them at temperatures close to the programming temperature as the material moves through its recovery. This is sometimes referred to as the "temperature memory effect". Using this method, researchers have been able to achieve a quadruple and even quintuple SMP effect. For instance, researchers prepared a semi-interpenetrating network composed of cross-linked poly(methyl methacrylate) (PMMA) and linear PEG. After polymerization the PMMA displayed a broad glass transition and the PEG had a sharp melt transition.[35] With these two separate phases they were able to program three shapes into the PMMA matrix and had one shape programmed into the PEG phase, creating the first example of quintuple shape memory. A second example from Luo and colleges used a living radical copolymerization with changing monomer feed ratios to create a compositional gradient along the polymer backbone.[36] This gradient resulted in a broad glass transition that yielded a multi-SMP capable of both quadruple and quintuple shape memory effects. We are aware of one previous example of a quadruple shape memory composite using three distinct thermal transitions, in contrast to broad thermal transitions as described above. Podgórski and colleagues used a combination of Michael-thiol and Michael/thiol-isocyanate layers in bi-layer and tri-layer structures that demonstrated triple and quadruple shape properties, respectively.[37] Using this method they obtained fixing and recovery ratios above 70% for all shape transitions. Intrinsically, this multilayer approach presents a limitation of multishape phenomena to the bulk, a limitation we sought to address in the present work.

Herein, we introduce the design of a multi-phase quadruple shape memory composite that displayed both bulk and surface quadruple shape memory behavior. We accomplished this by combining two fabrication methods that we previously reported to yield triple shape composites.[30,31] Briefly, we imbibed an electrospun PCL fiber mat with a PIPS precursor solution of PMMA dissolved in uncured epoxy liquid. Further processing led to a ternary composite with one permanent shape and capacity to program three temporary shapes locally or macroscopically. In what follows, we will explain the preparation, thermo-mechanical and quadruple shape memory properties of these composites.

2. Results and Discussion

Quadruple shape composites (4SMCs) were fabricated by combining two previously published methods to design triple shape polymeric composites as shown in Scheme 1.[30,31] We note that the depicted topology of the final 4SMC morphology has not been confirmed. In particular, we show the PMMA phase existing as a discrete "pockets", though a co-continuous

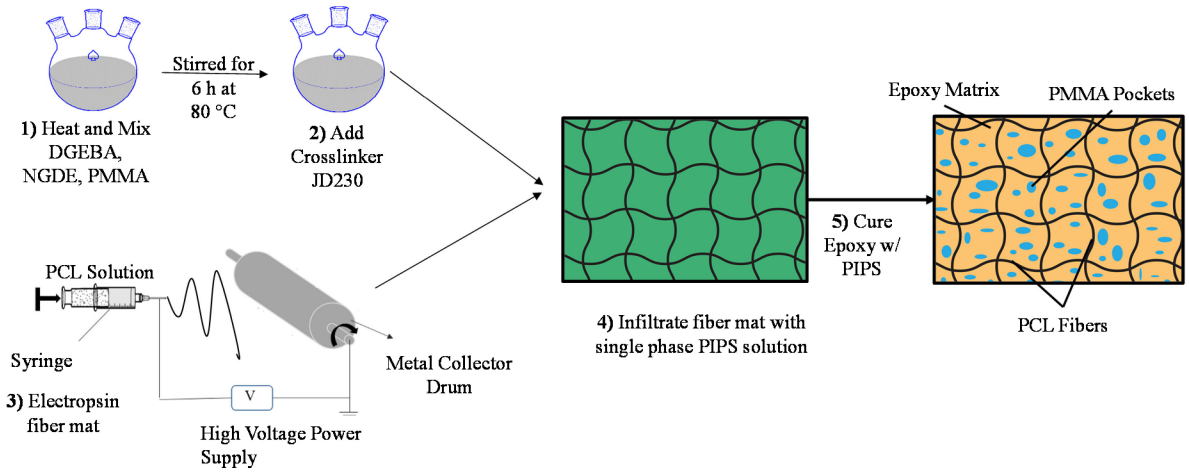

Scheme 1. Process to make 4SMCs. **1)** PIPS precursor is prepared by heating a solution of NGDE, DGEBA and PMMA at 80 °C until all materials formed a homogenous solution. **2)** JD230 cross-linker is then added and the solution was cooled to 50 °C. **3)** PCL web is separately prepared by electrospinning rotating collector drum. **4)** The PIPS precursor solution (green) is then imbibed into the web (black). **5)** Upon cure the PMMA and epoxy phase separate, creating a three-phase solid of PMMA, epoxy, and PCL.

morphology is possible. Several comparison compositions were prepared: (i) a triple shape composite of epoxy and PCL prepared by imbibing a solution of just the reactive epoxy liquid (monomers + crosslinker) into the PCL fiber mat, (ii) a triple shape PIPS composition consisting of phase-separated PMMA in epoxy, and (iii) pure epoxy resin. At the start of cure, all epoxy solutions were optically clear and fully transparent (Figure 1). At a critical point during cure the PIPS precursor solutions underwent phase separation with an accompanying dramatic optical change from transparent to opaque. This transition was observed to occur for both the neat epoxy/PMMA PIPS composition and the same matrix imbibed into the PCL web for the 4SMC material.

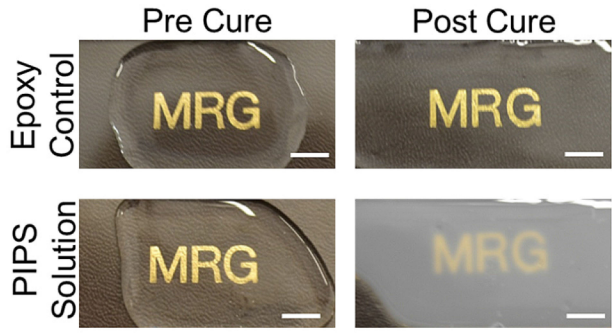

Figure 1. The images on the left are of epoxy liquids prior to cure. The top image is a pure epoxy resin and the bottom is a PIPS solution. After cure, the epoxy resin remained optically clear (shown top right) and the PIPS precursor solution became optically opaque (bottom right), indicating that phase separation had occurred. Scale Bar is 10 mm.

The thermal transitions of all composites and control materials were studied using differential scanning calorimetry (DSC). Calorimetric analysis using DSC revealed well separated glass and melt transitions in the composite materials indicating that multiple phases existed within the materials. The thermal transitions were compared using the second heating thermograms shown in Figure 2. The neat epoxy and PMMA samples (compositional controls) each showed a distinct glass transition (T_g) at 31 °C and 110 °C, respectively. The PCL control showed a distinct melting transition (T_m) at 55 °C. The triple shape polymeric composite (TSPC) showed both a step transition and a melting peak corresponding to the epoxy-rich phase with T_g at 34 °C and the PCL-rich phase with T_m at 55 °C, respectively. The triple shape PIPS composite showed two separate step transitions indicating the presence of the T_g of the epoxy at 31 °C and the PMMA at 102 °C, respectively. However, the step

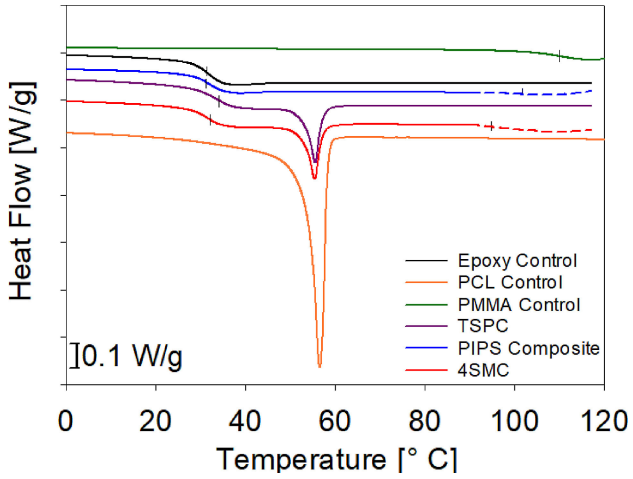

Figure 2. DSC thermograms (2nd heating) of 4SMCs, TS composite controls and material controls. Epoxy matrix, PCL and PMMA controls are shown in black, red and green respectively. The PIPS composite and TSPC controls are shown in blue and purple, respectively. The 4SMC is shown in red. The dashed lines are scaled up by a factor of 7 to make the PMMA T_g visible in the DSC traces. The heating rate was 10 °C/min for all samples.

transition of the PMMA phase was small compared to the epoxy which has been previously observed for other PMMA composite systems.[35] The 4SMC displayed 3 separate thermal transitions, the T_g of the epoxy at 32 °C, the T_m of the PCL at 55 °C and the T_g of the PMMA at 106 °C. For both the PIPS composite and the 4SMC the PMMA glass transitions were lower than that for the pure PMMA, indicating plasticization of the PMMA due to the epoxy monomers, likely due to incomplete phase separation. It is worth noting that this plasticization is less for the 4SMC than for the triple-shape PMMA-epoxy blend, leading us to speculate that the presence of PCL helped drive the phase separation, perhaps through affinity with PMMA.

The latent heat of melting of PCL was used to estimate the weight percentage of PCL in both 4SMCs and the epoxy/PCL TSMCs. We used the heat capacity step of the epoxy T_g to calculate the percentage of epoxy in the blends ("incorporation percentage of epoxy") by computing the ratio of that value to that of the pure epoxy control (0.074 $J g^{-1} °C^{-1}$). For both the PIPS composite and the 4SMC materials, the total percent composition for the PCL and epoxy phases were subtracted from 100% to estimate the incorporation percentage of PMMA. All calculated values are shown in Table 1. The calculated incorporation percentage of PMMA in PIPS composite was 25%, which exceeds the value measured during fabrication of 10%. This is likely due to incomplete phase separation,

Table 1. The measured thermal transitions and % compositions of all composite materials.

	Epoxy Tg[a]	Epoxy Incorporation[b]	PCL Tm[a]	PCL Incorporation[b]	PMMA Tg[a]	PMMA Incorporation[b]
TSPC	34.1	91	55.5	9	–	0
PIPS Composite	31.2	75	–	0	101.6	25
4SMC	32.0	79	55.4	9	94.8	12

[a] °C [b] %.

lowering the measured step change in heat capacity of the epoxy T_g.

The temperature-dependent dynamic mechanical properties of SMPs are a very important predictor of shape memory behavior, and provides useful information for deciding programming temperatures for different SMPs. The temperature-dependent transitions of all material composites are revealed in the DMA traces of Figure 3. The TSMC control displayed two

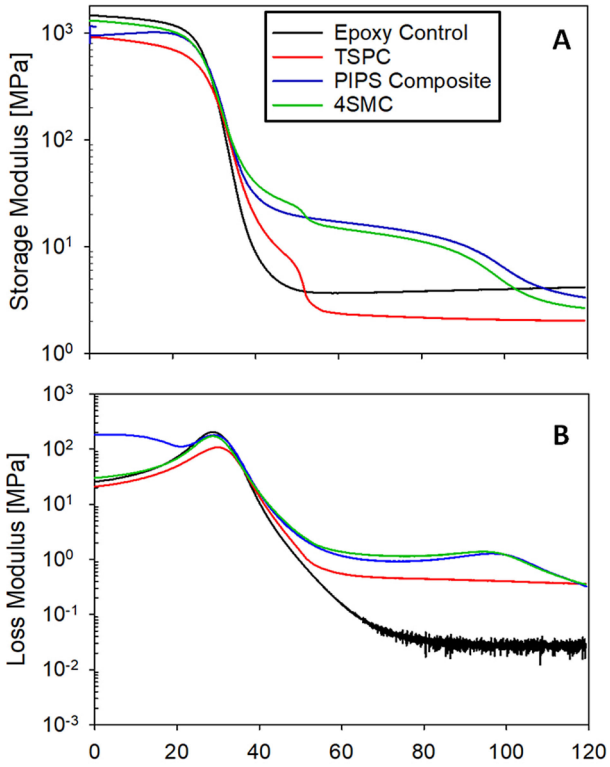

Figure 3. The DMA results for all material composites and an epoxy control. The top graph shows the temperature dependence of the storage modulus while the bottom shows the loss modulus. The thermal-mechanical transition of the PMMA was clearly visible. The heating rate for all tests was 2 °C/min

thermo-mechanical relaxations, one for the epoxy glass transition and one for PCL melting. The PIPS composite also displayed two thermal transitions, here for the glass transitions of the epoxy and PMMA phases. The glass transition events are evident most clearly in the loss modulus peaks at 29 and 98 °C, respectively. In contrast to the weak DSC signal, the mechanical signal associated with the glass transition of the PMMA phase in the composites was very clear. This strong mechanical signal shows clearly that the two material phases are well separated, indicating the possibility of mechanical programming (fixing) of two separate shapes, which will be explored below. The 4SMC composition showed three distinct thermal transitions in the DMA data, indicating that it should be able to fix three independent shapes.

Wide Angle X-ray Scattering (WAXS) experiments (Figure 4) were carried out to gain an understanding of the molecular packing of the fabricated composites. As expected from prior reports, the pure materials exhibited two (epoxy) and one (PMMA) amorphous halos. Very little x-ray diffraction has been done with epoxy materials making interpreting the two distinct halos difficult. However, PMMA has been extensively studied and the halo centered at $2\theta = 14^\circ$ is attributed to a well-defined average spacing of the PMMA side chains along the polymer backbone.[38,39] This apparently overlaps in length-scale with the average intermolecular (backbone) spacing of the same chains. PCL showed sharp peaks at $2\theta = 21^\circ$ and 23.6°, which correspond to d-spacings of 4.15 Å and 3.76 Å, respectively.

Such spacings are consistent with an orthorhomibic unit cell, with (110) and (200) lattice planes, respectively.[40–42] In the PIPS composite and in the 4SMC the PMMA amorphous halo was not clearly evident, but this may be due to relatively low sensitivity of WAXS. The 4SMC and the TSMC both showed the double amorphous halo attributed to epoxy and the crystalline domains for the PCL, indicating persistence of microstructure for these two phases in the composites.

To further examine the microstructure of the new composite materials, electron microscopy was utilized. In particular, SEM inspections of the surfaces and freeze-fractured cross-sections of all fabricated composites and an epoxy control were conducted, and representative results are shown in Figure 5. All composites, when compared to the neat epoxy, showed evidence of rough fracture surfaces when viewed in cross-section. The TSPC sample showed visual evidence of the PCL fibers on both the surface and the cross-section. The PIPS composite and 4SMC showed some uneven "pocketing," that may be attributed to the phase separation between the epoxy and PMMA phase. While these SEM observations are consistent with findings from WAXS experiments, their utility is limited due to inherent limitations associated with analysis of fracture surfaces. Transmission electron microscopy (TEM) with selective staining of particular phases should offer enhanced discernment potential and this is a goal for future work.

The shape memory behavior of all composite materials and an epoxy control is shown in Figure 6. Briefly, all SMC samples were heated above the thermal transition needed to program a shape into a specific "fixing" phase, for example epoxy, PCL, or PMMA. The programming temperatures for the epoxy, PCL and PMMA phases were selected to be slightly above associated T_g or T_m transitions, namely 40 °C, 70 °C and 120 °C, respectively. Once heated above the desired transition, each material was stretched and then cooled below the temperature transition to fix the temporary shape. This programming step was repeated once for the triple shape controls and twice for 4SMC. Once programming was completed, each material was heated at a continuous heating rate of 2 °C/min and the recovery events recorded as the tensile strain. For fixing of strains by vitrification of the epoxy and PMMA phases within the composites, samples needed only to be cooled below the associated T_g; however, for fixing of strains by PCL crystallization, samples were cooled to 0 °C to allow the PCL to fully crystallize. The individual steps are labeled in Figure 6 according to the procedural activity of that step in the cycle (stretching, cooling, or recovery) and the relevant material phase (epoxy, PCL, PMMA).

Figure 6A shows the one-way shape memory cycle (1WSMC) for the epoxy control which showed fixing and

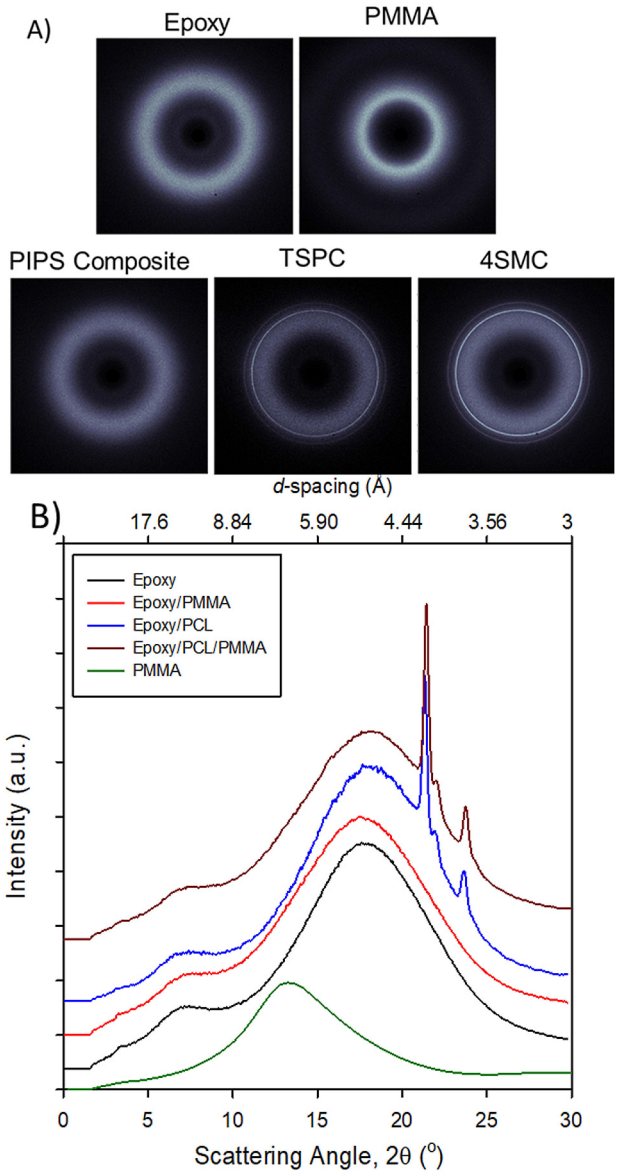

Figure 4. The Wide-Angle X-ray Diffraction of all control samples and composites. A) The WAXS scattering patterns for all materials B) The intensity versus diffraction angle for all tested materials.

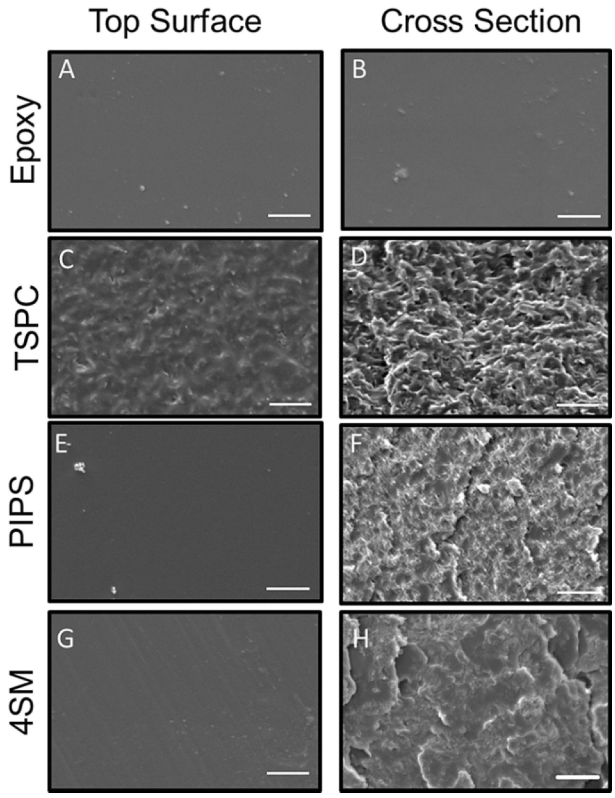

Figure 5. SEM of the composite materials and epoxy control. Images A, C, E, and G are representative images of the top surfaces of the epoxy control, TSPC, PIPS composite and 4SMC, respectively. Images B, D, F, H show the cross section of the epoxy control, TSPC, PIPS composite and 4SMC, respectively. Scale bar is 10 μm.

recovery ratios of 82% and 108%, respectively. (Note: a recovery ratio greater than 100% is sometimes observed due to thermal expansion effects.) The triple shape memory cycles (TSMCs) for the TSPC and PIPS composite are shown in Figure 6B and C, respectively. The TSMC showed a fixing ratio (R_f) for the epoxy and PCL phases of 92% and 93% and a recovery ratio (R_r) of 84% and 89%. The TSMCs for the PIPS composite showed a R_f for the epoxy and PMMA phases of 94% and 69%, and a R_r of 110% and 102%, respectively. The R_r being above 100% for both of the composites indicates some thermal shrinking as the material was mechanically cycled. The TSPC showed a stronger fixing capability compared to the PIPS composite for the higher temperature phase (PCL and PMMA, respectively), which was not evident in the 4SMC shown in Figure 6D–F. This higher fixing capability of the PCL phase for TSPC is attributed to the interconnectivity of the fibers being better able to resist the rubber elasticity of the matrix compared to the PMMA in the PIPS composite. This ability is diminished in the 4SMCs, which we attribute to the smaller incorporation level of PCL in those composites that naturally lessened the ability to resist the matrix contraction.

A summary of the R_f and R_r values for these 4SMCs is provided in Table 2. The epoxy phase of each material showed the strongest SM ability with R_f and R_r values over 95% for all tests. Both the PCL and PMMA phases showed a weaker fixing ability with R_f values ranging from 69–78%, however all calculated R_r values (for those strains programmed at temperatures associated with PCL and PMMA transitions) were found to exceed 99%. R_r values over 100% indicate that the material

Table 2. The fixing and recovery ratios for the 4SM composite cycled through three separate QSMCs.

	Epoxy		PCL		PMMA	
	R_f	R_r	R_f	R_r	R_f	R_r
Equal Strain	94.8	95.7	69.4	111.7	74.8	101.3
More PCL Strain	94.7	96.5	69.2	102.6	77.5	102.0
More PMMA Strain	94.7	96.1	78.1	102.7	68.9	99.2

All listed values are in units of percent.

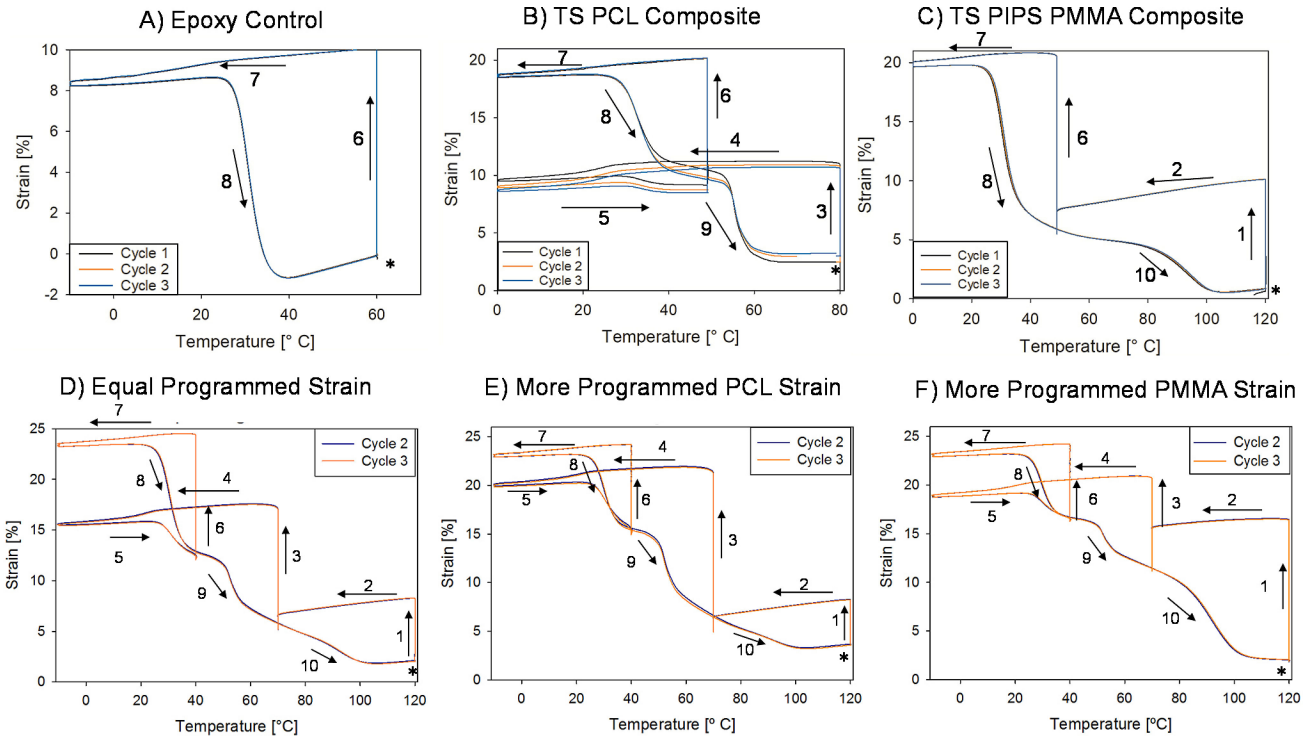

Figure 6. Shape memory characterization of epoxy matrix control and all composite materials. Graph A shows the 1 WSMC for the epoxy control matrix. In all graphs the asterisk denotes that starting point. Graph B and C show the triple shape memory cycles for the TSPC control and the PIPS composite control, respectively. Graph D, E and F are QSMCs programming different amounts of strain into each phase of the material. D: Equal amounts of strain were programmed into the composites and then recovered under continuous heating. E: More strain was programmed into the PCL phase of the material. F: More strain was programmed into the PMMA phase of the material. Step 1, 3, and 6 are stretching and programming strain into the PMMA, PCL and Epoxy phase respectively. Step 2, 4 and 7 were cooling steps with fixing of strain into the PMMA, PCL and epoxy phases, respectively. Steps 8, 9 and 10 show the recovery of the Epoxy, PCL and PMMA phases, respectively, under continuous heating. Step 5 was heating above the glass transition of the epoxy after cooling to a low temperature to fix the strain in the PCL.

recovered more strain than was fixed into that particular phase, and is likely due to some "cross-fixing" between phases. For instance, when the epoxy phase is strained some of that strain may be transferred to both the PCL or PMMA phases which are below their T_g. In contrast, straining the PMMA phase of the composites does not transfer strain to the PCL and epoxy phases since these materials are above their transition temperatures.

In Figure 7, we present a visual demonstration of the quadruple shape memory ability of our 4SMCs. For this demonstration, 3 temporary shapes were programmed into the 4SMC by heating the composite above the three separate transition temperatures, in the opposite order of the expected recovery. Since the first shape programmed was the last to be recovered, the first shape programmed was a "U" in the PMMA phase, followed by a "S" in the PCL phase followed by a temporary flat shape in the Epoxy phase. Then upon recovery, the 4SMC will transition from a flat shape, to an "S", to a "U" and then back to the permanent flat shape. Briefly, a strip of 4SMC was cut and heated above the glass transition of PMMA, to a temperature of 115 °C, using an oven. At this temperature, both the epoxy and PMMA phases are soft, while the PCL phase is molten. In this rubbery state, the sample was folded into a temporary "U" shape and fixed in that configuration with a binder clip. The sample was returned to the oven for an additional twenty minutes to give time for PMMA chains to relax and flow in response to the deformation, before cooling. Next, the folded sample was cooled in a freezer at −20 °C for 20 min and the clip then removed. While this temperature is well below the pertinent transition temperatures for all three components, the purpose was to vitrify the PMMA phase, establishing the "U" shape as that which was mechanically programmed into the PMMA phase. To observe the quality of this such mechanical programming, the sample was heated to T = 70 °C, a temperature exceeding T_g of epoxy and T_m of PCL (thus softening both phases), but below T_g of PMMA. A photograph of the sample was taken at this temperature. Heating to this temperature allowed any strain programmed into the PCL or epoxy phases to recover. These steps were repeated for the mechanical programming of strains the PCL and epoxy phases at T = 70 °C ("S" shape) and T = 45 °C (flat shape), respectively. In each case, the material was deformed to the desired shape, and the shape was held in place with binder clips. The material was returned to the oven once deformed for an additional 20 minutes at the programming temperature and cooled to −20 °C to fix the shape. In this way, the programming process was the same for each material component to ensure that any observed behavior was not a result of the programming conditions. As can be seen in Figure 7, the mechanical programming of shapes by PMMA vitrification ("U" shape) and

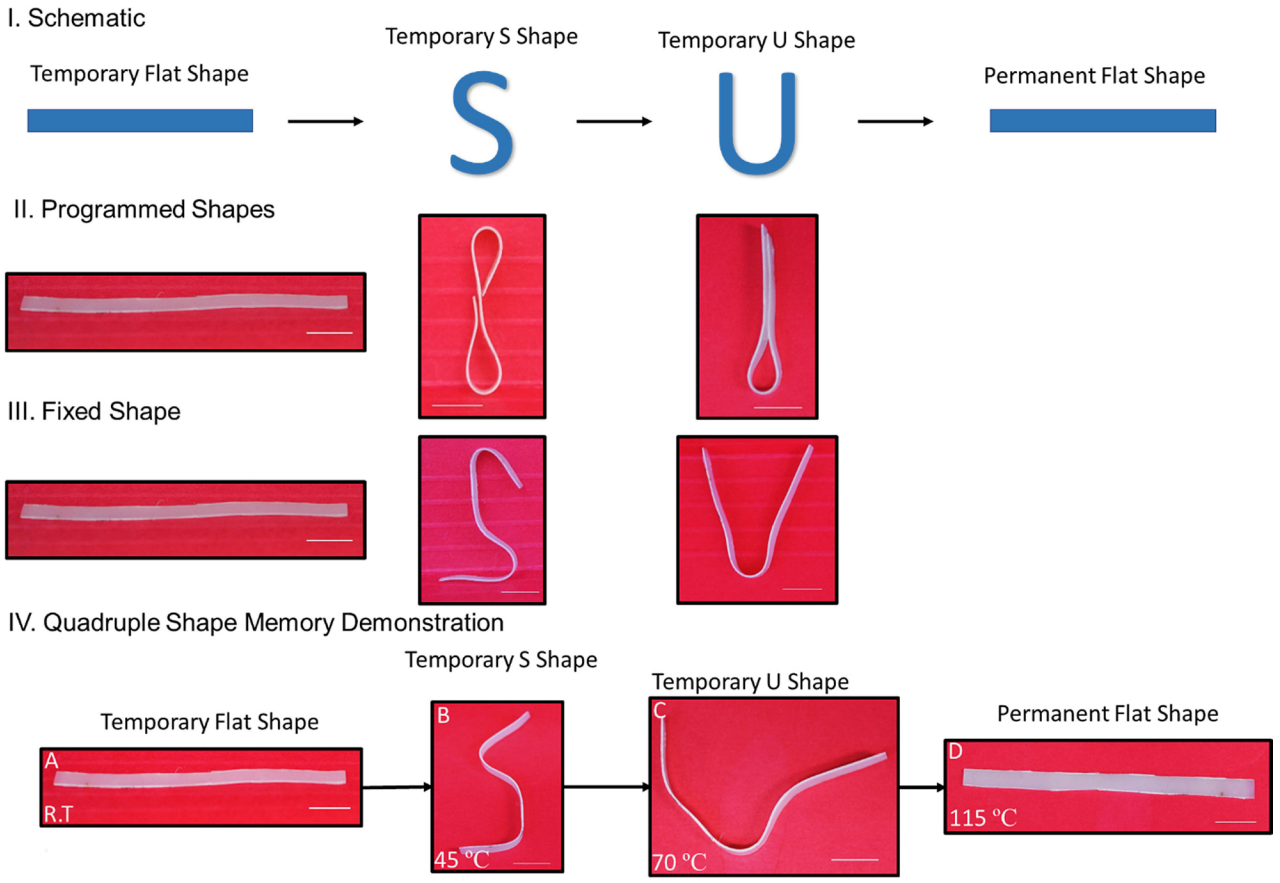

Figure 7. Macro SM Demonstration. I) shows an animation of the desired programmed shapes. II) Shows the programmed shapes in the 4SMCl. III) Shows the shapes fixed into the material by the desired material phase. IV) Shows the recovery of the 4SMCs the shape transitions from flat, to an S to a U to flat again, effectively demonstrating 4 distinct shapes. The scale bar shown in each image represents 10 mm.

PCL crystallization ("S" shape) was reasonable, though some of the programmed strain was lost in the process. This loss in strain is likely caused by some of the programmed shape being fixed into another phase of the material and then recovered when the 4SMC was heated above the transition temperature of the epoxy or PCL phases. Upon heating of samples with three separate shapes programmed into the three constituent phases, the 4SMC sample transformed spontaneously from a temporary flat shape, to an "S" shape, prescribed by the PCL phase, and then to a "U" shape, prescribed by the PMMA phase. Still further heating to 115 °C led to flattening back to the permanent (flat) shape, successfully demonstrating the ability to transition between three temporary shapes and one permanent one. A movie documenting the programming and recovery of these composites is included in the supplementary information.

While Figure 7 demonstrated bulk quadruple shape memory behavior of the 4SMC sample, surface shape memory – or reversible embossing – proved also to be possible. A visual demonstration of the quadruple surface shape memory (4SSM) behavior is shown in Figure 8. Here, a series of surface patterns were sequentially embossed on the surface of a 4SMC material using a simple glass-sandwich mold and a series of embossing steps at progressively lower temperatures. For this demonstration, we first cut a disk-shaped sample with a diameter of 16.5 mm (slightly smaller than a US penny). The 4SMC was stacked in contact with the "heads" side of the penny and the stack placed between two glass slides. Pressure was applied to the assembly using a set of large ACCO binder clips arranged with one along each edge of the glass slide, yielding an applied pressure of approximately 93 kPa distributed along the area of the glass slides. The assembly was then heated to 115 °C to soften all three phases of the 4SMC, leading to embossing (surface programming) of the penny surface shape into the PMMA phase by allowing the stress in that phase to relax completely over the course of 20 min. The sandwich was then cooled in a freezer at −20 °C, fixing the embossing by vitrifying the PMMA phase. The disk was then removed from the clamps and placed in the isothermal oven at 70 °C to allow any surface strain programmed into the PCL and epoxy phases to relax, but retaining the PMMA in its programmed state. These steps were repeated to program the horizontal lines into the PCL phase and the vertical lines into the epoxy phase at temperatures of 70 °C and 45 °C respectively. For each step, the disk was clamped against the tweezers, between two glass slides by two binder clips applying 93 kPa of pressure. The sandwich was place in the oven at 70 °C to program the horizontal lines into the PCL, then placed in the freezer at −20 °C to fix the shape

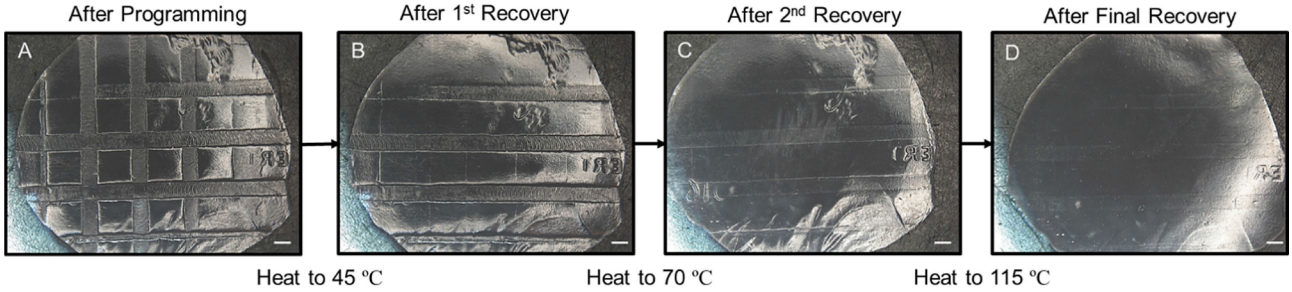

Figure 8. Surface Shape Memory Demonstration. A) Fully programmed disk with three separate patterns programmed on top of each other in the three separate material phases. B) 4SMC surface after allowing the epoxy to recover and the vertical lines fixed into the matrix recovered. C) 4SMC surface after triggering the PCL phase to recover and the horizontal lines recovered. D) 4SMC surface after triggering the PMMA to recover, returning the disk to its original shape. Scale Bar is 1 mm.

into the surface. The clips were removed and the sample heated to 45 °C to relax any strain programmed into the epoxy. We then clamped the sample against the tweezers at a 90 ° angle to the previous direction to program vertical lines into the epoxy. The sample was then heated to 45 °C and cooled to −20 °C to program and fix the surface pattern, respectively. Figure 8 shows the recovery of the surface shape patterns as the material is heated sequentially above the transition of the epoxy, PCL and PMMA phases, respectively. Figure 8A shows all three temporary surface patterns programmed into the material. Once the material is heated to 45 °C, the vertical lines programmed into the epoxy phase recovery, and the surface patterns left are the horizontal lines and the penny face (Figure 8B). The 4SMC disk is then heated above the T_m of PCL which allows the horizontal lines to recover (Figure 8C) and then finally above the T_g of the PMMA which allows the penny face to recovery (Figure 8D). As the surface shapes recovered some transitions, namely the PCL recovery did not show full surface shape recovery until heated above the transition temperature of the next material phase. This behavior was additionally observed for the macro shape memory demonstration and is due to some cross programming in the material phases with higher transition temperatures. At the end, not all of the penny face recovered likely due to some plastic deformation into the surface of the 4SMC disk.

To the best of our knowledge, this is the first demonstration of QSSM behavior. It is possible that the systems made by Luo[36] and Li[35] may have been capable of multi-shape memory behavior applied to surface embossing, given their broad transition behavior. However, such behavior was not reported. The laminated composite designed by Podgórski[37] would likely not be capable of QSSM, as not all material components are present on the surface. Our observed multi-shape memory embossing ability could prove to be highly relevant as topographical surface patterns have been proven to give material surfaces unique properties like adhesion,[43] antibacterial[44] and hydrophobic[45] properties. We postulate that with QSSM one could design a material composite that cycles through many different surface configurations with associated physical properties that could be tuned to a specific application.

In summary, this multiphase composite approach has proven to be a versatile and adaptable way to design new SMP systems that demonstrate both bulk and surface shape memory abilities. By combining an electrospun fiber mat with a triple shape PIPS solution we designed a 4SMC that demonstrated both quadruple bulk and surface shape memory behavior. However, one limitation is that the PIPS solution was very viscous and difficult to work into the fiber mats, indicating that this method may not work for incorporating additional material components, which would enable more material transitions.

3. Conclusions

To conclude, we have developed a new ternary composite, 4SMC, exhibiting quadruple shape memory properties. The new material was prepared by imbibing an electrospun web of PCL fibers with a single phase blend of PMMA in epoxy liquid, which underwent polymerization induced phase separation (PIPS) during epoxy cure to yield a three-phase composition. This new approach to the formation of ternary composites may be broadly applicable to other PIPS systems combined with electrospun webs, blown fibers, or foams. Our study of 4SMC thermomechanical behavior and morphological properties contrasted the new material with binary composite counterparts, revealing three distinct transitions well separated in temperature and promise of quadruple-shape memory. Indeed 4SMC was found to exhibit both bulk and surface shape memory behavior with one permanent shape and three temporary shapes. Such behavior may be useful for a wide range of applications. In addition, the design of these 4SMCs can be easily adopted to other applications by simply selecting different polymers for either the fibers or composite matrix, giving the 4SMCs new functions like drug delivery or reversible adhesion. Future work could include designing a 4SMC that responds to a variety of stimuli such as light or pH to increase the adaptability of these composites.

Experimental Section

All chemicals including diglycidyl ether of bisphenol-A (DGEBA), neopentyl glycol diglycidyl ether (NGDE), O,O′-Bis(2-aminopropyl) polypropylene glycol (Jeffamine D230) and poly(ε-caprolactone) (PCL) (nominal Mw = 90 000 g/mol) were purchased from Sigma-

Aldrich and used as received. PMMA (nominal Mw = 75 000 g/mol) was purchased from Scientific Polymer Products, Inc..

Electrospinning of PCL

The electrospinning solution was prepared by dissolving 2 g of PCL in 10 mL of a chloroform:DMF (Vchloroform:VDMF 8:2) solution and set to stir for 24 h, yielding a clear and colorless viscous solution. Electrospinning was conducted using a custom built set up that is composed of a high voltage power supply (Agilent E3630A), a syringe pump (KDS100, KD Scientific), a low voltage negative power supply (PS 500XT, Hoefer Scientific) and a 5 cm diameter rotating drum. Fiber mats were spun using a constant flow rate of 2 mL/h with an applied voltage of 12 kV at needle-collector distance of 10 cm. The fibers were collected on a negatively charged mandrel (−500 V) rotating at 800 rpm with a slow horizontal translation along the collecting drum axis (perpendicular to the electrospinning jet direction) to ensure that a uniform, randomly oriented fiber mat was produced.

Fabrication of PIPS Composites

PIPS composites were fabricated using previously reported methods.[31] Briefly, 20 g of 60:40 molar ratio of NGDE:DGEBA was added to a flask and 2 g of PMMA pellets subsequently added to yield a 10 wt-% solution of PMMA in liquid epoxy monomer. The flask was heated at 80 °C for at least 3 h under vacuum (to degas the solution) and magnetic stirring, resulting a single-phase viscous liquid. The cross-linker, Jeffamine-230, was then added to the solution, the temperature reduced to 70 °C and stirring continued for 15 min under continued application of vacuum. Next, the PIPS solution was poured into a Teflon™ casting mold with square rectangular bar-shaped cavities (80×80×1 mm) and transferred to a convection oven to cure the materials at 40 °C for 24 h and then 60 °C for 48 h, conditions previously found to yield complete cure as evidenced by post-cure calorimetric analysis.

Fabrication of Triple Shape Memory Composites (TSMCs)

TSMCs were fabricated using previously described methods.[30] Briefly, a 60:40 molar ratio of NGDE:DGEBA monomer solution was mixed together for 2 min. A 50 molar ratio of Jeffamine-230 was added to the solution and stirred for an additional 2 min. The solution was then imbibed into an electrospun PCL fiber mat and vacuum-infiltrated for 20 min. The composite was finally cured at 40 °C for 48 h, to prevent melting of the PCL fiber phase before matrix vitrification, and then 60 °C for 24 h to ensure complete cure.

Fabrication of Quadruple Shape Memory Composites (4SMCs)

A PMMA-based PIPS solution was first prepared as described above. When a homogeneous solution was obtained, a portion was poured first onto a glass slide, following which a PCL fiber mat was laid on top of it, partially absorbing the epoxy liquid. This approach was taken to minimize fiber melting, noting that the PIPS solution was prepared at a temperature exceeding the melt transition of the fiber mat. Imbibing of the PIPS solution was further advanced by hand manipulation until uniform translucency was achieved. Next, the composite was vacuum-infiltrated under an excess PIPS solution for 20 min to assure complete imbibing. Finally, the fiber mat was clamped between two glass slides, squeezing out a minor excess of PIPS solution, and cured at 40 °C for 24 h followed by 60 °C for 48 h. All materials, including 4SMC, PIPS Composite and TSMC, were prepared and cured using the same matrix solutions to minimize the potential for batch-to-batch variability.

Thermal Analysis

Thermogravimetric Analysis (TGA) was performed on all composite and control samples to characterize the thermal degradation of the materials. Such analyses were performed in high resolution mode to better capture the specific thermal degradation points. Samples were heated at a maximum rate of 50 °C/min with a resolution of 4 °C and a sensitivity of 1 to 600 °C. In this mode, the TGA ramped the temperature at a rate of 50 °C/min until temperature where the instrument detected mass loss, at which point the heating rate was decreased to capture fully the degradation event before continuing with the test.

Differential Scanning Calorimetry (DSC) was performed on all composite and control samples using a Q200 (TA instrument) equipped with a refrigerated cooling system. For each test, samples weighing 3–5 mg were loaded into a T-zero aluminum plan and first equilibrated by cooling to −50 °C. Samples were then heated at a rate of 10 °C/min to 120 °C and cooled at a rate of 5 °C/min to −50 °C, this initial heating being used to erase any thermal history. Samples were then heated by 10 °C/min to 120 °C to measure the glass transition (T_g) and melting transition (T_m) of the composite materials. The composition of all composite materials was measured using the heat of crystallization of the PCL and the stepwise change in heat capacity at T_g for the epoxy matrix. The material composition was estimated using Eqns. 1–3, and calculated values were compared to gravimetric values recorded during sample fabrication. Since the glass transition signal for PMMA was small, the PMMA composition was calculated by summing the % composition of the other material phases and then subtracted from 100 % (Eqn. 3).

$$W_{PCL}(\%) = \frac{\Delta H_{PCL-COMP}}{\Delta H_{PCL-pure}} * 100 \quad (1)$$

$$W_{epoxy}(\%) = \frac{\Delta C_{Pepoxy-COMP}}{\Delta C_{Pepoxy-pure}} * 100 \quad (2)$$

$$W_{PMMA}(\%) = 100 - W_{PCL} - W_{epoxy} \quad (3)$$

Dynamic Mechanical Analysis was used to measure the temperature dependences for all materials of the tensile storage modulus and the different thermal transitions via tensile loss modulus using a Q800 (TA Instruments). Samples featured variable dimensions with typical values of length, width and thickness of 6.25, 1.5, and 0.2 mm, respectively. The samples were first heated to 120 °C and then cooled at a rate of 2 °C/min to 0 °C to erase the thermal history of the sample. Samples were then heated at a rate of 2 °C/min to 120 °C while applying a small tensile deformation of 20 μm (0.4 %) at an oscillation frequency of 1 Hz.

Wide Angle X-ray Scattering (WAXS)

Wide-Angle x-ray (WAXS) was used to ascertain the molecular and nanoscale ordering of all materials. A Rigaku S-MAX3000 pinhole camera system with a MacroMax-200 generator operating with a Cu Kα emission (λ = 1.5406 Å) was employed for all x-ray experiments. WAXS patterns were collected using a generator voltage of 45 kV, current of 0.88 mA and a sample-detector distance of 122.7 cm. This resulted in a scattering angle range of $3^\circ < 2\theta < 40^\circ$ using Fujifilm image plates (CR HR-V) with a FujiFilm FLA7000

reader. Samples were exposed to achieve an adequate x-ray count for analysis, which was done using SAXSgui software v2.03.04.

SEM Analysis

All samples were examined for their microstructural features using a Scanning Electron Microscope JOEL 5600. To obtain surface images, small sample portions were cut from the base material and mounted onto SEM stubs. Cross-sections were obtained by cryo-fracturing the material in liquid nitrogen and mounting the broken section onto a microscopy stub. Both surface and cross sections were sputter-coated with gold for 45 s before imaging. Samples were imaged using an accelerating voltage of 8 kV and a spot size of 31.

Shape Memory Analysis

Shape memory cycles were performed on a Dynamic Mechanical Analyzer (TA Q800) operated in controlled-force mode. Briefly, each sample was first heated above the prescribed transition temperature and stretched at a rate of 0.05 N/min until the desired strain had been reached. Samples were then cooled at a rate of 2 °C/min to 0 °C and the force released at a rate of 0.1 N/min. Samples were then heated at a rate of 2 °C/min to record the shape recovery. For materials that held more than one shape, the programming step was repeated above each transition temperature (for 4SMCs, samples were stretched at 120 °C, 70 °C and 45 °C) until the desired number of independent shapes had been programmed in. The fixing (R_f) and recovery (R_r) ratios for each recovery event were then calculated using Eqns. 4 and 5.

$$R_f(x) = \frac{\varepsilon_x}{\varepsilon_{x,load}} \tag{4}$$

$$R_r(x \rightarrow y) = \frac{\varepsilon_x - \varepsilon_{y,rec}}{\varepsilon_x - \varepsilon_y}. \tag{5}$$

In Eqn. (4), ε_x, $\varepsilon_{x,load}$ are the strains measured after cooling and after unloading (thus, the strain fixed) and before unloading (thus attempted strain fixing). In Eqn. (5), additional terms include $\varepsilon_{y,rec}$, the strain achieved after recovery for shape y and ε_y, the strain before programming shape y (x can be a strain at 115 °C, 70 °C, 45 °C or 0 °C, the same holds for y). For strains programmed at 120 °C (strain programmed for PMMA-based fixing), ε_x was measured after the force had been removed from the sample and any strain allowed to recover at 70 °C. This ensured that the strain used in the calculations only accounts for the strain fixed by the PMMA phase. This was done for all programming steps.

Bulk quadruple shape memory behavior was further characterized using a visual demonstration. Samples were manually bent in an isothermal oven above their highest (PMMA-based) glass transition by folding the sample and clamping it down using a binder clip. For this step a glass slide was used as a spacer during bending steps to ensure the sample was not damaged. For the first programmed shape, the sample was heated above the transition of PMMA, 120 °C, and bent in the middle to program in a "U". Once bent, the sample was held for 20 min at 120 °C to allow the PMMA to flow into the desired shape and then cooled to −20 °C by placing in a freezer for 20 min. (Note: this low temperature was chosen out of convenience; any temperature below that of PMMA's T_g should have been sufficient.) The sample was photographed once taken out of the freezer and then heated to 70 °C (above all transitions except for the PMMA T_g) and photographed again. This allowed us to qualitatively compare the amount of strain attempted for programming into the material versus the amount actually programmed by vitrification of the PMMA phase. These steps were then repeated at 70 °C to program a "S" into the PCL network and then at 45 °C to program a temporary flat shape into the epoxy network.

Surface multi-shape memory was visually analyzed using two common surfaces as embossing masters: the face of a one cent US coin and the grooved pattern on a set of tweezers. To mechanically program the surface shape, each master was pressed against a circular 4SMC disk and uniform pressure was applied via two glass slides configured as a "sandwich". To apply pressure, the slides were clamped symmetrically with two binder clips and the sample held isothermally at 120 °C for 20 min in a convection oven. The full assembly was then moved to a freezer held at T = −20 °C to fix the first temporary surface shape via PMMA phase vitrification. These steps were repeated using surface embossing at 70 °C and 45 °C to program parallel lines – oriented perpendicular to each other – fixed by the PCL phase and epoxy phases, respectively. Samples were imaged using a Hirox 3D microscope (Model KH-8700), and each embossed image compared to the embossing master.

Acknowledgements

The authors acknowledge use of the facilities at the Syracuse Biomaterials Institute and the efforts of Dr. Eric Finkelstein in maintaining them. Partial support from the NSF IGERT (DOE-1068780), NSF DMR-1609523, and NSF DMREF (1334658) is gratefully acknowledged.

Conflict of Interest

The authors declare no conflict of interest.

Keywords: Phase Separation · Shape Memory Polymer · Electrospinning · Embossing

[1] C. Liu, H. Qin, P. T. Mather, *J. Mater. Chem.* **2007**, *17*, 1543.
[2] P. T. Mather, X. Luo, I. A. Rousseau, *Annu. Rev. Mater. Res.* **2009**, *39*, 445–471.
[3] M. D. Hager, S. Bode, C. Weber, U. S. Schubert, *Prog. Polym. Sci.* **2015**, *49–50*, 3–33.
[4] H. Meng, G. Li, *Polym. (United Kingdom)* **2013**, *54*, 2199–2221.
[5] T. Liu, T. Zhou, Y. Yao, F. Zhang, L. Liu, Y. Liu, J. Leng, *Composites Part A* **2017**, *100*, 20–30.
[6] Q. Zhao, M. Behl, A. Lendlein, *Soft Matter* **2013**, *9*, 1744–1755.
[7] H. Meng, G. Li, *Polymer (Guildf).* **2013**, *54*, 2199–2221.
[8] A. Lendlein, R. Langer, *Science* **2002**, *296*, 1673–6.
[9] A. Lendlein, *Science (80-.).* **2002**, *296*, 1673–1676.
[10] A. Lendlein, H. Jiang, O. Jünger, R. Langer, *Nature* **2005**, *434*, 879–882.
[11] H. Y. Jiang, S. Kelch, A. Lendlein, *Adv. Mater.* **2006**, *18*, 1471–1475.
[12] G. Li, G. Fei, H. Xia, J. Han, Y. Zhao, *J. Mater. Chem.* **2012**, *22*, 7692.
[13] X. Luo, P. T. Mather, **n.d.**, DOI 10.1039/c001295e.
[14] X. Gu, P. T. Mather, **2013**, *3*, DOI 10.1039/c3ra41337c.
[15] J. Mendez, P. K. Annamalai, S. J. Eichhorn, R. Rusli, S. J. Rowan, E. J. Foster, C. Weder, *Macromolecules* **2011**, *44*, 6827–6835.
[16] H. Lv, J. Leng, Y. Liu, S. Du, *Adv. Eng. Mater.* **2008**, *10*, 592–595.
[17] F. H. Zhang, Z. C. Zhang, C. J. Luo, I. T. Lin, Y. J. Liu, J. S. Leng, S. K. Smoukov, *J. Mater. Chem. C* **2015**, *3*, 11290–11293.
[18] R. Mohr, K. Kratz, T. Weigel, M. Lucka-Gabor, M. Moneke, A. Lendlein, *Proc. Natl. Acad. Sci.* **2006**, *103*, 3540–3545.
[19] E. D. Rodriguez, D. C. Weed, P. T. Mather, E. D. Rodriguez, D. C. Weed, P. T. Mather, **n.d.**, DOI 10.1002/macp.201300086.

[20] A. H. Torbati, P. T. Mather, *J. Polym. Sci. Part B Polym. Phys.* **2016**, *54*, 38–52.
[21] A. H. Torbati, R. T. Mather, J. E. Reeder, P. T. Mather, **n.d.**, DOI 10.1002/jbm.b.33107.
[22] E. D. Rodriguez, X. Luo, P. T. Mather, **n.d.**, DOI 10.1021/am101012c.
[23] M. Behl, M. Y. Razzaq, A. Lendlein, *Adv. Mater.* **2010**, *22*, 3388–3410.
[24] M. I. Lawton, K. R. Tillman, H. S. Mohammed, W. Kuang, D. A. Shipp, P. T. Mather, *ACS Macro Lett.* **2016**, *5*, 203–207.
[25] K. Inoue, M. Yamashiro, M. Iji, *J. Appl. Polym. Sci.* **2009**, *112*, 876–885.
[26] K. A. Burke, I. A. Rousseau, P. T. Mather, *Polymer (Guildf).* **2014**, *55*, 5897–5907.
[27] K. K. Westbrook, P. T. Mather, V. Parakh, M. L. Dunn, Q. Ge, B. M. Lee, H. J. Qi, *Smart Mater. Struct.* **2011**, *20*, DOI 10.1088/0964-1726/20/6/065010.
[28] J. Fan, G. Li, *RSC Adv.* **2017**, *7*, 1127–1136.
[29] I. Bellin, S. Kelch, R. Langer, A. Lendlein, *Proc. Natl. Acad. Sci.* **2006**, *103*, 18043–18047.
[30] X. Luo, P. T. Mather, *Adv. Funct. Mater.* **2010**, *20*, 2649–2656.
[31] A. H. Torbati, H. B. Nejad, M. Ponce, J. P. Sutton, P. T. Mather, *Soft Matter* **2014**, *10*, 3112–3121.
[32] H. B. Nejad, R. M. Baker, P. T. Mather, **n.d.**, DOI 10.1039/c4sm01379d.
[33] Y.-Y. Xiao, X.-L. Gong, Y. Kang, Z.-C. Jiang, S. Zhang, B.-J. Li, *Chem. Commun.* **2016**, *52*, 10609–10612.
[34] Z. He, N. Satarkar, T. Xie, Y. T. Cheng, J. Z. Hilt, *Adv. Mater.* **2011**, *23*, 3192–3196.
[35] J. Li, T. Liu, S. Xia, Y. Pan, Z. Zheng, X. Ding, Y. Peng, *J. Mater. Chem.* **2011**, *21*, 12213.
[36] Y. Luo, Y. Guo, X. Gao, B. G. Li, T. Xie, *Adv. Mater.* **2013**, *25*, 743–748.
[37] M. Podgórski, C. Wang, C. N. Bowman, *Soft Matter* **2015**, *11*, 6852–6858.
[38] R. L. Miller, R. F. Boyer, J. Heijboer, *J. Polym. Sci. Polym. Phys. Ed.* **1984**, *22*, 2021–2041.
[39] R. Lovell, A. H. Windle, *Polymer (Guildf).* **1981**, *22*, 175–184.
[40] B. Alvarado-Tenorio, A. Romo-Uribe, P. T. Mather, **2011**, DOI 10.1021/ma2005662.
[41] S. Nojima, K. Hashizume, A. Rohadi, S. Sasaki, *Polymer (Guildf).* **1997**, *38*, 2711–2718.
[42] Y. Chatani, Y. Okita, H. Tadokoro, Y. Yamashita, *Polym. J.* **1970**, *1*, 555–562.
[43] G. Huber, S. N. Gorb, N. Hosoda, R. Spolenak, E. Arzt, *Acta Biomater.* **2007**, *3*, 607–610.
[44] K. Glinel, P. Thebault, V. Humblot, C. M. Pradier, T. Jouenne, *Acta Biomater.* **2012**, *8*, 1670–1684.
[45] H. Teisala, M. Tuominen, J. Kuusipalo, *J. Nanomater.* **2011**, *2011*, 1–6.

Manuscript received: April 26, 2018
Accepted Article published: June 19, 2018
Version of record online: July 4, 2018